ELSEVIER

Chemical Engineering Journal 125 (2006) 119–126

Chemical Engineering Journal

www.elsevier.com/locate/cej

Mass transfer characteristics of a novel three-phase airlift contactor with a semipermeable membrane

Babak Jajuee, Argyrios Margaritis *, Dimitre Karamanev, Maurice A. Bergougnou

Department of Chemical and Biochemical Engineering, Faculty of Engineering, University of Western Ontario, London, Ontario, Canada N6A 5B8

Received 5 September 2005; received in revised form 19 August 2006; accepted 23 August 2006

Abstract

The effects of hydrocarbon contaminants and solid loading on gas–liquid volumetric mass transfer coefficient, $K_{\mathrm{L}}a$, were studied in a three-phase 25 l concentric cylindrical airlift contactor with a semipermeable membrane. The porous membrane could retain a large volume of immobilized solid particles and enhanced mass transfer and mixing in the airlift contactor. A specific form of the continuity equation was combined with gas holdup values in order to set up an expression for the mass transfer coefficient calculation. Water with different hydrocarbon concentrations of 0–200 mg/l *p*-xylene and 0–25 mg/l naphthalene were used as liquid media, under varying solid loadings and superficial gas velocities. The results indicated that deviation of mass transfer coefficient could go either way when hydrocarbons were dissolved in water: the most significant reduction in $K_{\mathrm{L}}a$ occurred at the concentration of 37 (mg/l) for *p*-xylene after which $K_{\mathrm{L}}a$ recovered and increased slightly. A less severe depression of $K_{\mathrm{L}}a$ was observed for naphthalene. Total solid loading in the airlift contactor was limited to the maximum amount of solid entrapped within the porous textile membrane. Higher superficial gas velocity resulted in the increase of the effect of solid loading on $K_{\mathrm{L}}a$.

Keywords: Mass transfer; Hydrodynamic; Airlift contactors; Hydrocarbon contamination; Solids immobilization

1. Introduction

Airlift reactors are a special type of multiphase pneumatic contactors widely used in chemical and biotechnological process industries. The design of airlift contactors has undergone extensive modifications by proposing a myriad of configurations to improve the hydrodynamic and mass transfer characteristics, which in turn are the subjects of much research interest. In general, airlift contactors are distinguished by two vertical sections: aerated and non-aerated zones. One of these zones sparged by a gas is the riser in which higher gas holdup leads to a difference in the bulk density of gassed liquid compared to that of downcomer and induces fluid circulation: upflow in the riser and downflow in the downcomer. The self-generated liquid circulation caused by hydrostatic pressure differences gives airlift contactors additional advantages to bubble columns such as intensive circulation of liquid in the entire reactor, lower energy consumption, higher heat-transfer rate and homogeneous shear [1–3]. Nevertheless, airlift contactors are pneumatically agitated devices characterized by fluid circulation in a defined cyclic pattern through channels, and thus their inherent plug flow characteristics make longer mixing time and relatively smaller volumetric mass transfer rate compared to conventional bubble columns [4–6]. In a development the impermeable membrane was replaced with a semipermeable one (permeable to liquid and impermeable to gas bubbles) in order to improve the rate of mass transfer and reduce the mixing time by producing the both vertical (upward in the riser and downward in the downcomer) and horizontal flow pattern through the draft tube from the downcomer to the riser [3]. The resulting airlift contactor shows great significance for biotreatment of recalcitrant pollutants dissolved in water owing to the capability of immobilizing microorganisms to the porous membrane and improved rate of oxygen mass transfer [7,8]. Attachment of microorganisms to a fixed support divides airlift bioreactor systems into discrete phases. The liquid phase of such systems has viscosities close to water while in conventional bioreactor systems suspended microbial cultures in liquid phase cause higher liquid viscosities and lower mass transfer rates.

One of the most widely spread environmental recalcitrant pollutants that causes serious environmental hazards in aqueous system is diesel fuel. Diesel fuels are very complex mixtures of many individual compounds, most with carbon numbers between 10 and 22.

---

* Corresponding author. Tel.: +1 519 661 2146; fax: +1 519 661 3498.
E-mail address: amarg@uwo.ca (A. Margaritis).

1385-8947/$ – see front matter © 2006 Elsevier B.V. All rights reserved.
doi:10.1016/j.cej.2006.08.020

Nomenclature

a	specific interfacial surface (m^2/m^3)
c	concentration (mol/m^3)
H	height (m)
U_{sg}	superficial gas velocity (cm/s)

Greek symbols

α, β	constant
ε	holdup
θ	time (s)
μ	viscosity (Pa s)

Subscripts

c	continuous phase
d	dispersed phase
g	gas
i	interface
L	liquid

Benzene, toluene, ethyl benzene, xylenes (BTEX) and polyaromatic hydrocarbons (PAHs) are the key water-soluble chemical constituents of diesel fuels. Several members of this family of chemicals are considered toxic, carcinogenic, mutagenic, and teratogenic. BTEX are of the greatest concern on account of their higher solubility in water compared to aliphatic hydrocarbons.

Biotreatment of dissolved hydrocarbons in the modified airlift contactor is based on activation of a presumably well-adapted microbial consortium in contaminated soil [8]. After an acclimation period, appropriate microorganisms that are capable of degrading the target pollutant cluster naturally around soil particles. These particles can be used for developing the microbial consortium and also supporting the biofilm of this consortium [9]. Attachment of particles to a fixed support minimizes the friction between them and prevents them from leaving the reactor while it makes the stimulation of the indigenous microorganisms much easier (higher metabolic activity) by introducing nutrients and oxygen into the attached soil particles. Moreover, several layers of immobilized cells on a support provide greater resistance to toxicity. To provide a larger and more even area of immobilized cells per unit volume of the contactor, the draft tube was replaced with a semipermeable wall in the present work. The primary objective of this study was to characterize the oxygen mass transfer and hydrodynamics of such a modified airlift contactor by monitoring the effects of immobilization of sand particles in the presence of *p*-xylene and naphthalene as the representatives of monocyclic and polycyclic aromatic hydrocarbons, respectively. The results will be of importance in using this apparatus as an airlift bioreactor for biotreatment of recalcitrant hydrocarbon pollutants.

2. Theory

A synopsis of different mechanisms of mass transfer from gas bubbles into the bulk of liquid in gas–liquid contactors have been reviewed by Jajuee et al. [10]. Mass transfer models are generally developed from the equation of continuity, which describes an overall material balance for a component over a fixed volume element in space, through which the component is flowing. These models predict the mass transfer behavior in systems of varying complexity. Models of higher complexity incorporate more terms of the continuity equation to offset errors incurred by the film theory in practical systems. From a practical standpoint, it will suffice here to consider the terms of molecular diffusivity, bulk motion in one direction, and non-steady state change of concentration to set up the following expression for measuring experimental mass transfer data [10]:

$$\ln \frac{c_{A,i} - c}{c_{A,i} - c_{A0}} = \frac{(-K_L a)\theta}{1 - \varepsilon_g} \tag{1}$$

where K_L is the rate of mass transfer, a the specific surface area, c the time-dependant molar concentration of species A, and ε_g is the volume fraction of gas bubbles in the bulk of the liquid. Since air–water interface is incessantly replenished in a high surface renewal rate, Eq. (1) is grounded on the assumption that bulk motion drives eddies and liquid particles in a continuous circulation in this airlift contactor. Holdup values can be simply given by:

$$\varepsilon_g = \frac{\Delta H}{\Delta H + H_L} \tag{2}$$

where H_L and ΔH represent the ungassed liquid height and the increase in liquid level after gassing, respectively. In view of the fact that holdup is affected by the induced liquid circulation which in turn depends strongly on geometry, holdup values are hardly comparable with other authors' results although the techniques used in literature is quite similar [11]. Gas holdup is found to depend on superficial gas velocity at fixed sparging diameter. Godbole et al. [12] proposed the following correlation for gas holdup in Newtonian solutions:

$$\varepsilon_g = 0.255 U_{sg}^{0.6} \mu^{-0.19} = \alpha U_{sg}^{\beta} \tag{3}$$

Owing to the generation of larger bubbles with shorter residence time and higher terminal velocity, larger sparging diameters reduce holdup at fixed gas flowrate. In water, as the diameter increases from 0.5 to 3 mm, exponent β in Eq. (3) decreases from 1 to 0.79 and constant α from 2.8 to 0.76 [13].

3. Experimental

3.1. Description of apparatus

Experimental data were obtained in a modified airlift contactor with a working volume of 25 l whose dimensions are listed in Table 1. The column was a cylindrical glass tube divided by a rectangular sheet of non-woven polyester textile that was supported by stainless steel mesh (1 cm opening, wire diameter 0.8 mm). Fig. 1 shows the experimental set up. The airlift contactor was mounted on a stainless steel platform. The thickness of the textile membrane was 1.5 cm and its porosity was 0.995. Unlike rigid porous materials, non-woven textile

Table 1
Apparatus dimensions

Internal diameter of column, D_c (m)	0.145
Height of column, H (m)	1.8
Liquid height in column, h (m)	1.7
Width of membrane (m)	0.145
Length of membrane (m)	1.46
Thickness of membrane (m)	0.01
Bulk density of membrane (g/cm^3)	9.73
Porosity of membrane	0.995
Depth of D.O. probe from top (m)	0.25 and 1.2
Number of holes in sparger	20
Diameter of holes (m)	0.001

has no pores with a determined length and diameter. The non-woven structure of the membrane allows wide range of solid particle distribution from 1 μm to 2 mm to get entrapped and fixed in space. It was required that the materials used in this study would not absorb hydrocarbon molecules or react with them. Nor do they lose these compounds by diffusion. In this regard, a Teflon–aluminum diaphragm gas pump (KNF Inc.) with adjustable airflow rate was used for aeration of the contactor. All tubing for transferring contaminated water or gas circulation was stainless steel or specially formulated Tygon tubing (Masterflex, F-4040-A). The air was distributed through a perforated stainless steel tube with 20 holes of 0.5 mm. The sparger was placed at a height of 10 cm above the bottom of the tank. Deionized water was used for the bulk phase and the water level above the membrane (top clearance) and under the membrane (bottom clearance) was kept 11 cm unless otherwise stated. The gas phase in this experiment comprised air and nitrogen for aeration and deaeration, respectively. Gas flowrates were measured by a set of calibrated rotameters. The aerated cross-sectional area of the contactor was used in order to calculate the superficial gas velocity. The data of dissolved oxygen concentration was measured by using a polarographic probe (Orion 850 Inc.) and the data collection software. A thin Teflon membrane was used to reduce the 95% response time of the probe to 15 s to practically eliminate the effect of response time on mass transfer coefficient in Eq. (1). The temperature was kept constant at 20 ± 1 °C for all experiments.

3.2. Choice of materials

Deionized water and mixtures of water, *p*-xylene, and naphthalene (*p*-xylene 99% and naphthalene 99%, Sigma–Aldrich, Milwaukee, WI) were used for the continuous phase. Having low solubility in water, naphthalene was first dissolved in *p*-xylene and then added to deionized water. To investigate the effect of

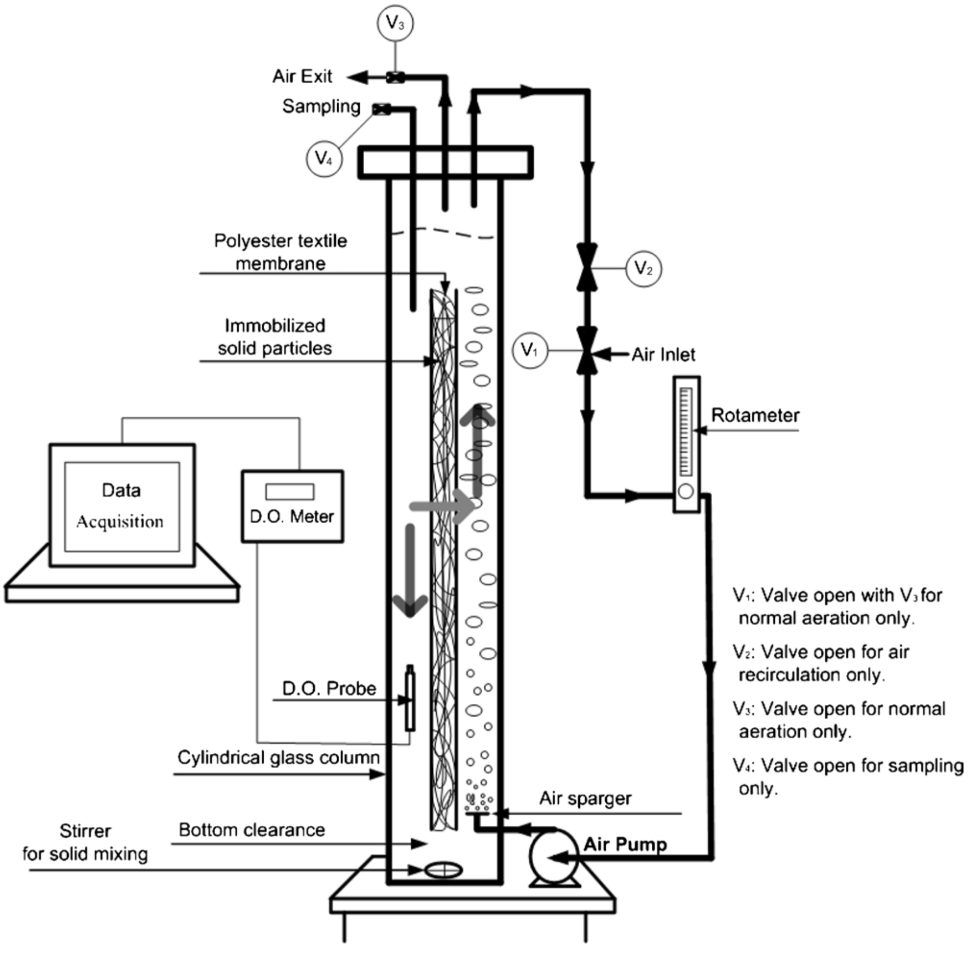

Fig. 1. Diagram of experimental apparatus.

immobilization of sand particles on oxygen mass transfer, silica (SiO_2 white quartz, Sigma–Aldrich) with different particle size distribution was used.

3.3. *Experimental procedure*

3.3.1. *Mass transfer in pure water*

In the first place, oxygen mass transfer data were obtained in the absence of sand particles and hydrocarbon contaminants in the contactor. The rate of mass transfer was measured in different vertical locations along the downcomer region. In order to optimize the rate of oxygen mass transfer, the effects of the following variables were studied: superficial gas velocity, bottom and top clearance of textile membrane, and the number of textile layers. After oxygen removal by sparging nitrogen gas, the column was aerated and dissolved oxygen (D.O.) concentration was measured using the polarographic oxygen probe. The volumetric oxygen mass transfer coefficient, K_La, was determined by the dynamic method based on Eq. (1). The mean gas holdup was obtained by measuring the liquid heights of aerated and unaerated parts using a graduated vertical scale.

3.3.2. *Mass transfer in contaminated water*

The mixtures of deionized water, *p*-xylene, and naphthalene were prepared in Pyrex reagent bottles of 20 l with Teflon-stoppers. The concentration of *p*-xylene and naphthalene in water was measured by elution technique and gas chromatography (GC). The GC used in this study was a Varian CP-3800 gas chromatograph equipped with a splitless injection port, a flame ionization detector, and a chrompack capillary column (CP-Sil 5 CB column) of 25 m length, 0.53 mm internal diameter, and a film thickness of 5 μm. The chromatographic conditions for this study were as follows: injection port temperature, 275 °C; initial column temperature, 35 °C, initial time, 0.5 min; heating rate, 15 °C/min; final time, 10 min; final temperature, 300 °C; detector temperature, 325 °C; helium (carrier gas) flowrate, 3 ml/min. Bottles and other glassware used for sampling were soaked in a sodium hydroxide solution for several hours, then rinsed with deionized water, dilute nitric acid, more deionized water, and finally dried overnight at 110 °C. Samples were taken by a syringe made of durable glass and feature large chrome-plated metal Luer lock tips that could efficiently dispense large volumes of hydrocarbon solutions. Glass hypovials of 25 ml with screw caps seal and Teflon septa were used for sampling. Great care was needed not to leave any headspace in the samples. Five millilitres of each sample was drawn with a micropipette and 2 ml of dichloromethane and metafluorotoluene, also known as the eluent and the internal standard, respectively, were added. Thereupon capped vials with a headspace of 3 ml were placed horizontally in a Magni-Whirl shaker for 10 min and upside down for another 10 min at room temperature (20 ± 1 °C) to complete phase separation. A 10 μm gastight syringe was used to inject manually 1 μm of the eluent of each sample into the GC instrument to measure the hydrocarbon concentrations. To build a standard calibration file for the two compounds of interest, a solution of methanol, *p*-xylene and naphthalene was prepared in a glass vial of 40 ml. Standards included five glass vials of 25 ml containing 20 ml of deionized water and different volumes (in microliter range) of the forgoing methanol solution. The elution technique for standards and samples was the same. The calibration curve was prepared using five standards to assure the accuracy of the measurements. The concentrations of samples were obtained from linear regression of the resulting calibration curve. A sealed re-circulation system was used for gas phase to prevent volatile hydrocarbons from leaving the contactor, as shown in Fig. 1. The mass transfer data were obtained in the same way explained before for pure water.

3.3.3. *Mass transfer and soil immobilization*

Generally speaking, soil immobilization is a process of retaining soil particles in pores. The horizontal bulk motion exploited by hydrostatic pressure differences between the aerated section and unaerated section of the textile membrane is, in effect, responsible for entrapment of suspended particles. The transport mechanisms of solid particles entrapped in the textile membrane are composed of diffusion, interception, and sedimentation [14]. Pure silica sand with a wide range of size distributions was used to study the effect of solid particle immobilization on oxygen mass transfer rate. The particle size analyzer Mastersizer (Malvern Instruments Ltd., Worcestershire, UK) was employed for size analysis. The carrier fluid was doubly distilled water with a refractive index of 1.33. The refractive index for the sample was set to 1.51. The particle size distribution was stabilized with ultrasonication. No agglomeration of the sample was detected. Two different particle size fractions of 1–100 μm, and 100–1000 μm were studied. After a certain time of hydrodynamic steady state conditions, silica sand from each fraction was introduced intermittently to the contactor and the effect of soil immobilization on mass transfer was studied. Finally the amount of immobilized sand particles on the membrane was determined by drying the membrane at 110 °C, and separating the attached sand particles.

4. Discussion of experimental results

The specific configuration of the airlift contactor with porous membrane renders higher mass transfer rates up to 80% compared to classic airlift contactors with non-porous membranes [3]. The porous structure and high permeability of the textile wall allows the bulk of liquid to pass horizontally through it, while the small sizes of pores preclude passage of gas bubbles. Moreover, the horizontal flow caused by hydrostatic head provides higher mixing values, characteristic of CSTR reactors, while fluid circulation in a cyclic pattern on the both sides of the textile preserves the advantages of plug flow reactors. In this airlift contactor, however, mass transfer rate could be improved by selecting an appropriate location for textile wall. Fig. 2 encompasses a wide range of mass transfer data measured in two different locations of 25 cm and 120 cm from the top of the downcomer. Mass transfer data was obtained using Eq. (1) in conjunction with the data of gas holdups shown in Fig. 3. Each data point in Fig. 2 represents an average value of 10 different runs with the standard deviation of 10%. It can be seen that K_La was very similar for every position of the probe in

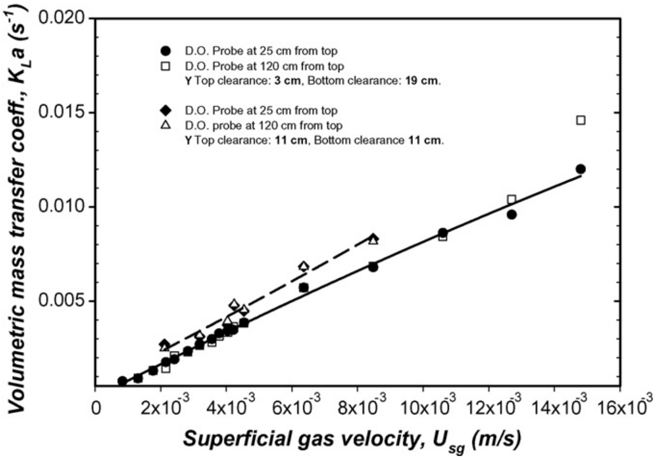

Fig. 2. K_La values vs. superficial gas velocity at different locations of downcomer with the standard deviation of 10%.

the downcomer, suggesting a perfectly mixed system in the contactor. The mass transfer data were collected first when the top and bottom clearances of the textile wall were 3 cm and 19 cm, respectively. Thereafter, the both top and the bottom clearances changed to 11 cm. It was proved that the equal clearance of 76% of the length of the membrane, which was 11 cm for this airlift contactor, would suffice to provide proper water circulation, and higher mass transfer rate up to 20%, as shown in Fig. 2. On that account, Fig. 4 shows the effect of bottom and top clearance on mass transfer coefficient for two different superficial gas velocities of $U_{sg} = 6.36$ mm/s and $U_{sg} = 4.25$ mm/s. In this experiment, the top clearance was kept constant at 12 cm, while the bottom clearance changed from 0 to 14 cm. As bottom clearance increased from 0 to 12 cm, mass transfer coefficient increased by 20%. Fig. 4 illustrates that increasing bottom clearance more than 12 cm had no effect on mass transfer coefficient. The effect of the thickness of the textile membrane on mass transfer was studied at two different superficial gas velocities. The results, not shown here, suggested that higher mass transfer drop occurs for lower superficial gas velocity when increasing the thickness of membrane.

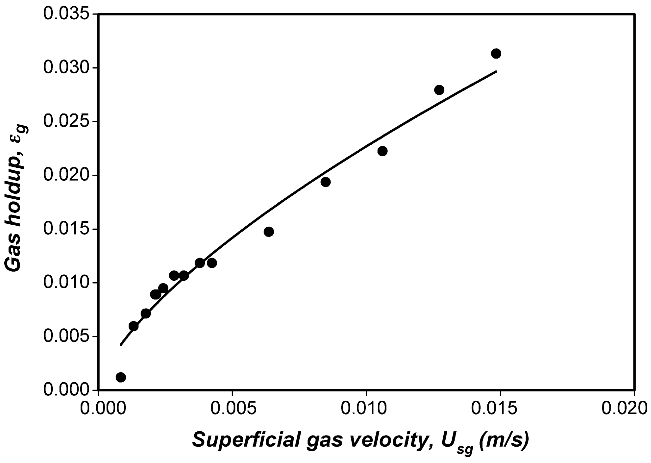

Fig. 3. Gas holdup vs. superficial gas velocity with the standard deviation of 14%.

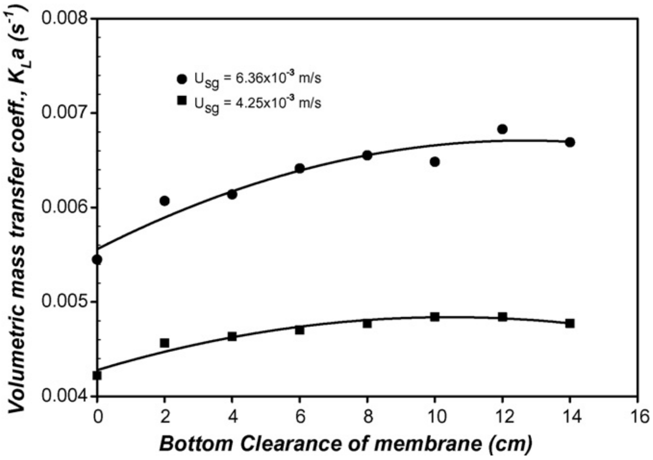

Fig. 4. Volumetric mass transfer coefficient vs. bottom clearance with the standard deviation of 8%.

There is a substantial body of data in the literature on the effect of surfactants on mass transfer rate [12,15–20]. The term of surface-active is referred to molecules that are composed of groups of opposing solubility tendencies, typically an oil-soluble hydrocarbon chain and a water-soluble ionic moiety. It should be noted that hydrocarbon compounds are not surfactants although some structurally dissimilar groups within their molecules, e.g. –CH_3 group in xylenes, might increase their solubility, and hence affect surface tension and mass transfer. To improve the physical properties, however, surfactants may be added to some oil fuels. The measures required to purify air/water systems are so difficult that the presence of surface-active contaminants in most systems of practical importance is inevitable. Therefore, in order to inspect the effect of *p*-xylene and naphthalene on mass transfer rate and diminish the effect of surfactants, the experiments were carried out under analogous and uniform conditions. The concentrations of *p*-xylene and naphthalene approached to equilibrium with time, as shown in Fig. 5. The decrease in concentration resulted from the physical adsorption of these compounds on the textile membrane. Naphthalene is less soluble in water than *p*-xylene and gets physically adsorbed to less extent

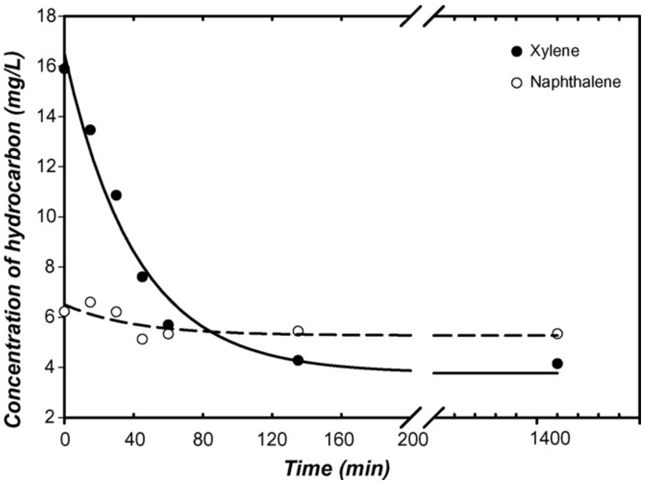

Fig. 5. Reduction in concentration of hydrocarbons due to physical absorption on textile membrane with the standard deviation of 14.5%.

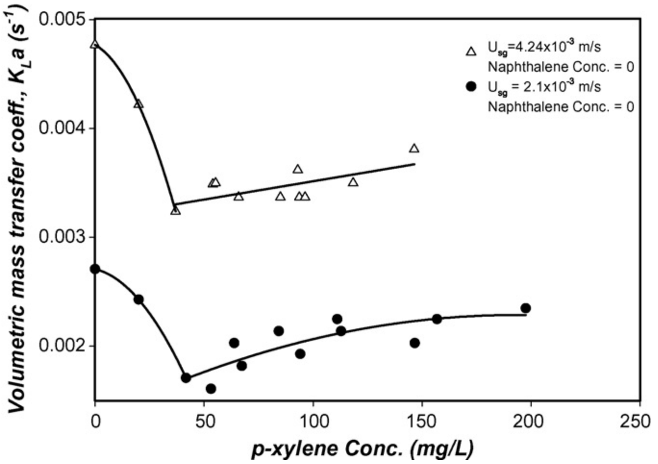

Fig. 6. Effect of dissolved *p*-xylene on volumetric mass transfer coefficient. The data points have the standard deviation of 21%.

on the textile membrane. Therefore, naphthalene concentration did not decrease in water as much as *p*-xylene concentration did. The adsorption of *p*-xylene and naphthalene on the membrane was 16.2 mg/g and 2.7 mg/g, respectively. Fig. 6 shows the effect of *p*-xylene on mass transfer coefficient for $U_{sg} = 4.25$ mm/s and $U_{sg} = 2.10$ mm/s. It can be seen that the mass transfer coefficient decreased drastically and then increased gradually. Severe reduction in volumetric mass transfer coefficient followed by a much softer trend of K_La increase has been observed by other authors and detailed theoretically by Jajuee et al. [21]. As it was pointed out before, naphthalene was first dissolved in *p*-xylene and the mixture of the two hydrocarbons was introduced to water to improve the rate of solubility of naphthalene crystals in water. Fig. 7 illustrates the mass transfer coefficient for these solutions at a constant concentration of 76 mg/l for *p*-xylene. It can be seen that traces of contaminants in aqueous systems could have a profound effect on mass transfer behavior. The reduction in mass transfer rate, though imperceptible, can be attributed to interfacial resistances. Such justification draws the marked analogy between dissolved hydrocarbons and other surface contaminants in eliminating significantly the internal circulation of gas bubbles and reducing drastically the overall mass transfer rate [12,15]. However, the amount of impurity may be so small that there would be no measurable change in the bulk of fluid properties. Systems that exhibit high interfacial tensions, e.g. air/water systems, are most subject to such effects. By the fact that the both amount and type of contaminants are important in determining their influence [12], accounting for the effect of impurities is quiet complicated. In general, contaminants can affect mass transfer via hydrodynamic and molecular effects [12,15–19]. The interaction between these two interfacial phenomena can perforce increase or decrease the mass transfer rate. Hydrodynamic effects are mobility of the interface that may be enhanced through the action of the local surface tension gradients caused by small differences in concentration along the interface. Contaminants can mainly affect the motion of and transfer from bubbles by changing the mobility of all or part of the interface. During the course of mass transfer, movements at the interface result from local variations of interfacial tension, which in turn have been ascribed to variations in interfacial concentration, temperature and electrical properties [17]. Interfacial motion, however, tends to increase the rate of mass transfer above that which would occur in the absence of interfacial motion [18]. Interfacial motion, whether caused by forced flow or hydrodynamic effects, is thereby changed by introducing contaminants. Since surface tension changes are large for air/water systems, contaminants play a particularly important role in these systems [12,15,16,19]. Molecular effects, as the second cause of mass transfer alternation, are interfacial resistances whose magnitude depends upon the nature of the transferring substances and the contaminants [16]. Surface resistances may arise from the interaction of surface contaminants with the species being transferred. For air bubbles in water, the ratio of μ_d/μ_c is so small that little viscose resistance exists to internal circulation of bubbles, while at large ratios of μ_d/μ_c, say, water drops in air, the viscous resistance of the internal fluid limits internal motion of water drops even for pure systems. Therefore, the drag, terminal velocity and mass transfer are more sensitive to the presence of contaminants for systems of lower μ_d/μ_c because contaminants tend to damp out internal motion of the dispersed phase by rendering the interface rigid for such systems [22]. When contaminants are added to a system undergoing mass transfer, they can reduce the interfacial tension. In addition, contaminants may cause a resistance or surface viscosity to motion at the interface. Based on laboratory measurements of gas-transfer and free-surface hydrodynamics for various interfacial conditions, the interfacial tension appears to be a critical process in air–water gas exchange [19,20].

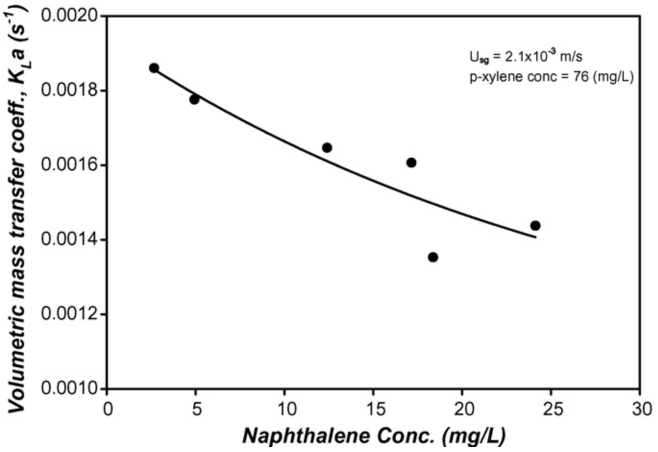

Fig. 7. Effect of naphthalene dissolution on volumetric mass transfer coefficient. The data points have the standard deviation of 10%.

Referring to the capability of the porous medium in entrapping soil particles, it was of value to inspect the effect of soil immobilization on mass transfer. Fig. 8 shows size distribution of the two particle fractions used for this study. The first group of particles with the size range of 1–100 μm covers the size range of microorganisms and the second group with the particle size from 100 to 1000 μm represents soil particles composed of indigenous microorganisms. The total amount of sand particles immobilized from the first and the second groups per unit volume of the membrane were 0.007 g/cm^3 and 0.24 g/cm^3, respectively. Immobi-

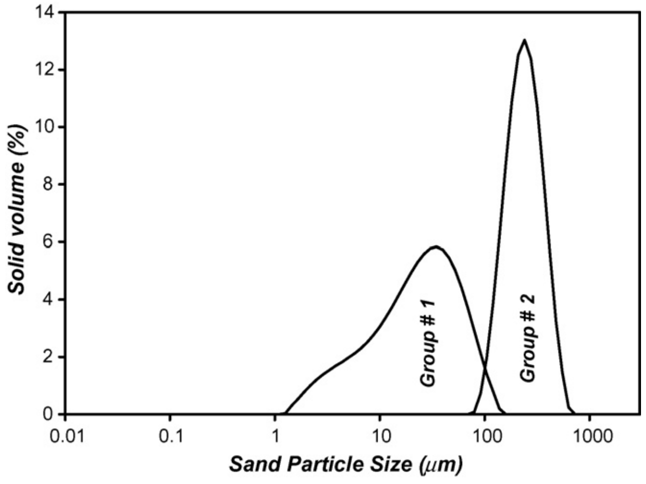

Fig. 8. Size distribution of the two particle fractions used for this study.

lization of the first group of particles had no effect on mass transfer. At superficial gas velocities of $U_{sg} = 4.25$ mm/s and $U_{sg} = 1.30$ mm/s, mass transfer remained constant at $0.005\ s^{-1}$ and $0.001\ s^{-1}$, respectively, with standard deviation of 16%. Fig. 9 shows the effect of sand immobilization from the second group on mass transfer coefficient. At superficial gas velocities of $U_{sg} = 4.25$ mm/s, $U_{sg} = 2.10$ mm/s, and $U_{sg} = 1.30$ mm/s, mass transfer drop due to maximum loading of 3.7% (volume of solid particles/volume of contactor) was 23%, 15%, and 7%, respectively. It should be borne in mind that solid loading for both fractions was continued to the point that no more particles could be immobilized on the membrane. Lower mass transfer drop due to immobilization of sand particles at lower superficial gas velocities augurs well for biodegradation of recalcitrant hydrocarbons whose volatilization before being biodegraded is a major problem that should be deterred. Worded differently, the airlift contactor appears to have higher performances at lower superficial gas velocities owing to the major role of porous membrane in mixing. This matter is of paramount importance when dealing with volatile hydrocarbon contaminants. Higher superficial gas velocities result in higher oxygen mass transfer generally desired in most water-based biotechnologies. However, in case of treating highly volatile hydrocarbons high superficial gas velocity helps these chemicals escape from the bioreactor. The kinetics of biodegradation of dissolved volatile hydrocarbons and removal efficiency of the airlift contactor with semipermeable membrane has been studied elsewhere [8]. More pronounced analysis of the mechanism of soil immobilization and hydrodynamics of this contactor have been reviewed [23,24].

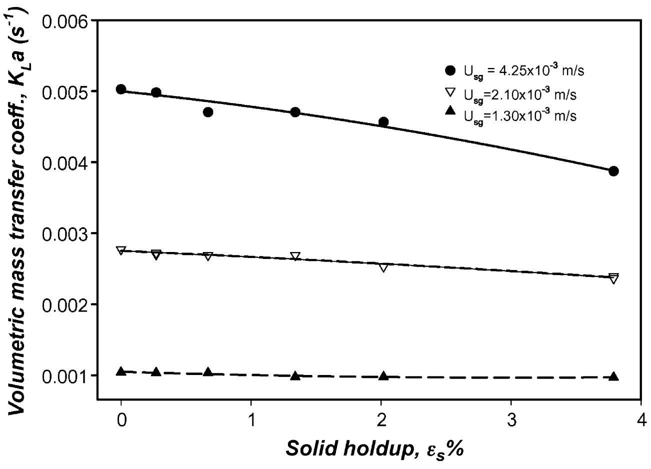

Fig. 9. Effect of solid holdup on volumetric mass transfer (second group of solid particles) with the standard deviation of 13%.

5. Conclusion

Aside from being a function of the superficial gas velocity and gas holdup, $K_L a$ is strongly affected by the permeability of the polyester textile membrane in the airlift contactor through changing the liquid circulation velocity and mixing rate. When *p*-xylene and naphthalene were dissolved in water they caused contamination of the gas–liquid interface, which affected the interfacial surface tension and the volumetric mass transfer coefficient, $K_L a$. The observed mass depletion rates due to solid immobilization in the textile membrane were higher for higher superficial gas velocities. In other words, at lower superficial gas velocities the $K_L a$ values were independent of solid particle concentrations. Further, $K_L a$ increased as gas superficial velocity increased at a given constant solids holdup. By inference, this airlift contactor evinces higher mass transfer efficiency for lower superficial gas velocities where lower liquid circulation velocity and mixing rate can be compensated by horizontal flows through the porous membrane.

Acknowledgments

The authors are grateful to Imperial Oil Ltd. and Natural Sciences and Engineering Research Council (NSERC) of Canada for financial assistance of the research. B. Jajuee wishes to acknowledge Western Engineering Scholarship.

References

[1] R.A. Bello, C.W. Robinson, M. Moo-Young, Gas holdup and overall volumetric oxygen transfer coefficient in airlift contactors, Biotechnol. Bioeng. XXVII (1985) 369–381.

[2] E.E. Peterson, A. Margaritis, Hydrodynamic and mass transfer characteristics of three-phase gaslift bioreactor systems, Crit. Rev. Biotechnol. 21 (4) (2001) 233–294.

[3] D.G. Karamanev, C. Chavarie, R. Samson, Hydrodynamics and mass transfer in an airlift reactor with a semipermeable draft tube, Chem. Eng. Sci. 51 (7) (1996) 1173–1176.

[4] P. Verlaan, A.M.M. Van Eijs, J. Tramper, K. Van't Riet, K.Ch.A.M. Luyben, Estimation of axial dispersion in individual sections of airlift-loop reactor, Chem. Eng. Sci. 44 (1989) 1139–1146.

[5] P. Weiland, U. Onken, Differences in behaviour of bubble columns and airlift loop reactors, Ger. Chem. Eng. 4 (1981) 174–181.

[6] P. Weiland, U. Onken, Fluid dynamics and mass transfer in an airlift fermenter with external loop, Ger. Chem. Eng. 4 (1981) 42–50.

[7] D.G. Karamanev, C. Chavarie, R. Samson, Hydrodynamics of soil immobilization in the immobilized soil bioreactor, AIChE J. 43 (5) (1997) 1163–1170.

[8] B. Jajuee, A. Margaritis, D. Karamanev, M.A. Bergougnou, Kinetics of biodegradation of *p*-xylene and naphthalene and oxygen transfer

in a novel airlift immobilized bioreactor, Biotechnol. Bioeng. (2006) doi:10.1002/bit.21106, in press.

[9] M.P. Otte, J. Gagnon, Y. Comeau, N. Matte, C.W. Greer, R. Samson, Activation of an indigenous microbial consortium for bioaugmentation of pentachlorophenol/creosote contaminated soils, Appl. Biochem. Biotechnol. 40 (6) (1994) 926–932.

[10] B. Jajuee, A. Margaritis, D. Karamanev, M.A. Bergougnou, Application of surface renewal-stretch model for interface mass transfer, Chem. Eng. Sci. 61 (2006) 3917–3921.

[11] M.Y. Chisti, M. Moo-Young, Airlift reactors: characteristics, applications and design considerations, Chem. Eng. Commun. 60 (1987) 195–242.

[12] S.P. Godbole, A. Schumpe, Y.T. Shah, Hydrodynamics and mass transfer in non-Newtonian solution in a bubble column, AIChE J. 30 (2) (1984) 213–220.

[13] J.M.T. Vasconcelos, J.M.L. Rodrigues, S.C.P. Orvalho, S.S. Alves, Mendes, R.L. Mendes, A. Reis, Effect of contaminants on mass transfer coefficients in bubble column and airlift contactors, Chem. Eng. Sci. 58 (2003) 1431–1440.

[14] E.H. Hsu, L.T. Fan, Experimental study of deep bed filtration: a stochastic treatment, AIChE J. 30 (2) (1984) 267–273.

[15] J.J. Jeng, J.R. Maa, Y.M. Yang, Surface effects and mass transfer in bubble column, Ind. Eng. Chem. Process. Des. Dev. 25 (1986) 974–978.

[16] D.R. Raymond, S.A. Zeiminski, Mass transfer and drag coefficients of bubbles rising in dilute aqueous solutions, AIChE J. 17 (1) (1971) 57–65.

[17] E.S.P. de Ortiz, H. Sawistowski, Stability analysis of liquid–liquid systems under conditions of simultaneous heat and mass transfer, Chem. Eng. Sci. 30 (12) (1975) 1527–1528.

[18] J.T. Davies, E.K. Rideal, Interfacial Phenomena, Academic Press, New York, 1963, pp. 235 and 295–296.

[19] S.P. McKenna, W.R. McGillis, The role of free-surface turbulence and surfactants in air–water gas transfer, Int. J. Heat Mass Transf. 47 (2004) 539–553.

[20] V. Linek, M. Kordac, T. Moucha, Mechanism of mass transfer from bubbles in dispersions. Part II. Mass transfer coefficients in stirred gas–liquid reactor and bubble column, Chem. Eng. Process. 44 (2005) 121–130.

[21] B. Jajuee, A. Margaritis, D. Karamanev, M.A. Bergougnou, Influence of dissolved hydrocarbons on volumetric mass transfer coefficient in a novel airlift contactor, Chem. Eng. Sci. 61 (2006) 4111–4119.

[22] R. Clift, J.R. Grace, M.E. Weber, Bubbles, Drops, and Particles, Academic Press, New York, 1978, pp. 174–199.

[23] D.G. Karamanev, R. Samson, High-rate biodegradation of pentachlorophenol by biofilm developed in the immobilized soil bioreactor, Environ. Sci. Technol. 32 (1998) 994–999.

[24] B. Jajuee, A. Margaritis, D. Karamanev, M.A. Bergougnou, Experimental studies and CFD simulation of liquid velocity and gas holdup in an airlift contactor with semipermeable membrane, AIChE J., 2006, in press.